

1 **SEARCH FOR THE STANDARD MODEL HIGGS BOSON IN THE DECAY**
2 **MODE $H \rightarrow \gamma\gamma$ WITH ATLAS**

3 R. TURRA

4 on behalf of the ATLAS Collaboration

5 *Dipartimento di Fisica, Università degli studi di Milano, Via Celoria 16,*
6 *20133 Milano, Italy*

7 This article summarizes the search for the Standard Model Higgs Boson in proton-proton collisions with the ATLAS detector at the LHC in the diphoton channel. The data used correspond to an integrated luminosity of 4.8fb^{-1} collected with the ATLAS detector at a centre-of-mass energy of $\sqrt{s} = 7\text{TeV}$ and 5.9fb^{-1} at $\sqrt{s} = 8\text{TeV}$. In the diphoton mass range 110–150 GeV, the largest excess with respect to the background-only hypothesis is observed at 126.5 GeV, with a local significance of 4.5 standard deviations. Taking the look-elsewhere effect into account in the range 110–150 GeV, this significance becomes 3.6 standard deviations. The Standard Model Higgs boson is excluded at 95% confidence level in the mass ranges of 112–123 GeV and 132–143 GeV.

8 **1 Introduction**

9 The Higgs mechanism is one of the best-motivated processes to explain electroweak symmetry breaking. In the Standard Model (SM), this mechanism explains the generation of the W and Z boson masses and predicts the existence of the only elementary scalar in the SM, the Higgs boson.

10 The $H \rightarrow \gamma\gamma$ decay has a quite small branching ratio (2.2×10^{-3} for $m_H = 120\text{GeV}$), a small signal-over-background ratio but a very simple signature and a good resolution. The channel is sensitive to the Higgs boson in the low mass range up to $\sim 140\text{GeV}$ and it is the one with largest expected sensitivity to a SM Higgs boson up to $m_H = 125\text{GeV}$. The main backgrounds are the irreducible background, coming from the QCD production of two isolated prompt photons, and the reducible background, produced in jet events in which at least one jet is misreconstructed as an isolated photon.

11 The ATLAS detector² consists of an inner tracking detector surrounded by a superconducting solenoid providing a 2 T magnetic axial field, electromagnetic and hadron calorimeters, and a muon spectrometer. The main subdetectors relevant to the search presented here are the calorimeters, in particular, the electromagnetic section, and the inner tracking system. The inner detector provides tracking in the pseudorapidity region $|\eta| < 2.5$ and consists of silicon pixel and microstrip detectors inside a transition radiation tracker. The electromagnetic calorimeter, a lead liquid-argon sampling device, is divided in one barrel ($|\eta| < 1.475$) and two end-cap ($1.375 < |\eta| < 3.2$) sections. The barrel ($|\eta| < 0.8$) and extended barrel ($0.8 < |\eta| < 1.7$) hadron calorimeter sections consist of steel and scintillating tiles, while the end-cap sections ($1.5 < |\eta| < 3.2$) are composed of copper and liquid argon.



30 2 Dataset

31 Two dataset are analysed, the first from 2011 data at $\sqrt{s} = 7 \text{ TeV}$ the second from 2012 data
32 between January and June at $\sqrt{s} = 8 \text{ TeV}^1$. The corresponding integrated luminosities are
33 4.8 fb^{-1} and 5.9 fb^{-1} . The main difference is the pileup condition, for example the mean number
34 of interactions per bunch crossing is 9.1 for 2011 and 19.5 for 2012.

35 3 Reconstruction and selection

36 Photons are reconstructed from electromagnetic clusters and classified as converted or un-
37 converted looking at the matching between tracks and clusters in the pseudorapidity region
38 $|\eta| < 2.37$, excluding the calorimeter barrel-to-end-cap transition regions $1.37 < |\eta| < 1.52$.
39 The photon energy is measured from energy deposits in the three longitudinal layers, corrected
40 for calibration constants computed with Monte Carlo (MC) samples. Converted photon are
41 measured using also the conversion point. The final value of the energy is corrected with scale
42 factors depending on η and typically of the order of 1 % applied to the calibrated photon energy
43 as obtained from studies using $Z \rightarrow ee$ decays in data. With respect to the previous analysis
44 tracking, vertexing and matching to cluster have been improved for the 2012 dataset to ensure
45 that the reconstruction of converted photons is robust against pileup.

46 Two energetic, well identified and isolated photons are required. The cut on the transverse
47 energy, E_T , is 40 GeV for the leading candidate, 30 GeV for the second. Because of the high
48 background from jets, a powerful jet rejection is needed. In 2012 a cut-based method using
49 shower shape parameters is applied: the middle layer of the electromagnetic calorimeter and
50 the hadronic calorimeter are used to reject jets and wide showers and the fine segmentation
51 of the first compartment of the electromagnetic calorimeter is used to separate photons from
52 neutral high momentum pions decaying in a very collimated couple of photons. In 2011 a
53 similar selection is performed using a neural network technique. The photon reconstruction and
54 identification efficiency ranges typically from 65 % to 95 % for E_T in the range 25 to 80 GeV.
55 The isolation is computed from the energy contained in a cone around the photon candidate
56 ($\Delta R = \sqrt{(\Delta\eta)^2 + (\Delta\phi)^2} < 0.4$, where $\Delta\eta$ and $\Delta\phi$ are the aperture in the pseudorapidity
57 and azimuthal direction). The core region of the electromagnetic cluster is excluded from the
58 calculation. The isolation is corrected for the photon energy lateral leakage inside the cone and
59 for the mean ambient energy. In the 2012 analysis this quantity has been improved to be more
60 robust against the position of the proton bunch in the proton beam. The isolation cut retains
61 87 % of Higgs boson signal events with $m_H = 120 \text{ GeV}$ while rejecting 44 % of the selected data,
62 which includes jets that can be misidentified as photons.

63 After selection 23788 (35271) diphoton candidates are selected in the 2011 (2012) dataset.

64 4 Categorization

65 To improve the sensitivity to the search the candidates are classified in various categories with
66 different signal-to-background ratio and different invariant mass resolution using: the presence
67 in the event of two jets with a vector boson fusion (VBF)-like topology, the η direction of the
68 two photons in the calorimeter, the conversion status of the photons, the p_{Tt} defined as the
69 orthogonal projection of the diphoton momentum on the thrust axis defined as the direction
70 of the vectorial difference between the transverse momenta of the photons. The variable p_{Tt}
71 is strongly correlated with the diphoton transverse momentum, but it has a better detector
72 resolution. The goal of the two-jets category is to select Higgs produced through the VBF
73 mechanism where two forward jets are produced with little QCD radiation in the central region.

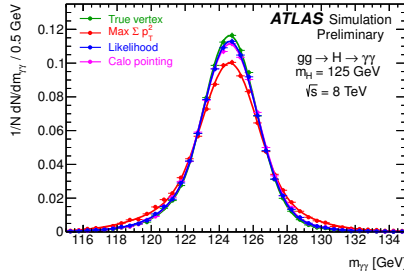


Figure 1: Distribution of the expected diphoton mass for $H \rightarrow \gamma\gamma$ signal events as a function of the algorithm used to determine the longitudinal vertex position of the hard-scattering event¹.

74 5 Mass computation and primary vertex

75 The invariant mass is computed from the two photon energies and their opening angle. This
 76 last quantity is improved with the estimation of the primary vertex using the direction of the
 77 photons measured thanks to the longitudinal segmentation of the electromagnetic calorimeter.
 78 The selection of the primary vertex is also relevant for the selection of the jets associated with
 79 the hard interaction.

80 The primary vertex of the hard interaction is identified using a likelihood with various inputs:
 81 the directions of flight of the photons as determined by the measurements using the longitudinal
 82 segmentation of the calorimeter, the average beam spot position, and the $\sum p_T^2$ of the tracks
 83 associated with each reconstructed vertex. In case of the 2011 dataset, the conversion vertex is
 84 also used in the likelihood for converted photons with tracks containing silicon hits. As shown in
 85 Fig. 1 the calorimeter information (with a resolution of $\sigma_z \sim 15$ mm using only the calorimeter
 86 pointing, and $\sigma_z \sim 6$ mm for two converted photons with silicon hits, if the vertex information
 87 is used) is sufficient to improve the mass resolution and is very close to the optimal resolution
 88 that can be achieved by using the true hard scattering primary vertex position. The mass
 89 resolution is similar when the likelihood is used to select the primary vertex. The addition of
 90 the tracking information from the inner detector is necessary to improve the identification of
 91 the hard-interaction primary vertex needed for the jet selection.

92 6 Background and signal models

93 For the statistical analysis of the measured diphoton spectrum, the background is parametrized
 94 by an analytic function for each category, where the normalization and the shape are obtained
 95 from fits to the diphoton invariant mass distribution. Different parametrizations are chosen
 96 for the different event categories to achieve a good compromise between limiting the size of a
 97 potential bias introduced by the chosen parametrization and retaining good statistical power.
 98 The background modelling uncertainties are estimated by checking how accurately the chosen
 99 model fits different predicted diphoton mass distributions and comparing different functional
 100 forms for the background model using high statistics MC samples.

101 Higgs boson production and decay are simulated with several MC samples that are passed
 102 through a full detector simulation. The MC Higgs signal diphoton mass distributions are fitted
 103 using a model consisting in a Crystal Ball plus a small Gaussian. A fit to the Higgs boson mass
 104 shapes is performed on the distributions given by the MC samples. The main systematics for the
 105 signal model are the photon identification efficiency affecting the signal yield, the calorimeter
 106 energy resolution uncertainty and the photon energy scale affecting the mass resolution.

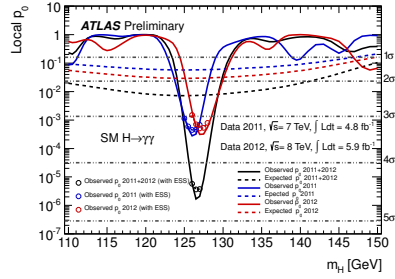


Figure 2: Expected and observed local p_0 values for a SM Higgs boson as a function of the hypothesized Higgs boson mass m_H for the combined analysis and for the $\sqrt{s} = 7$ TeV and $\sqrt{s} = 8$ TeV data samples separately. The observed p_0 including the effect of the photon energy scale uncertainty on the mass position is included via pseudo-experiments and shown as open circles¹.

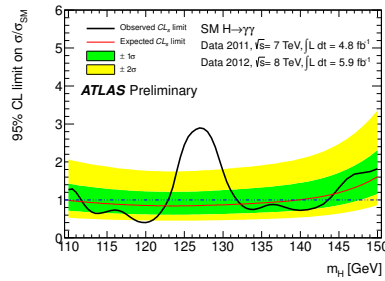


Figure 3: Expected and observed CLs limit on the normalized signal strength as a function of the assumed Higgs boson mass for the combined analysis.¹

107 7 Results

108 The statistical approach used for this analysis is the modified frequentist approach (CLs).³ The
 109 combined likelihood function is the product of the likelihood functions for the 10 categories. The
 110 95% confidence level limit on of the inclusive production cross section of a SM-like Higgs boson
 111 relative to the SM cross section, is shown on Fig. 2. In the diphoton mass range 110–150 GeV,
 112 the largest excess with respect to the background-only hypothesis is observed at 126.5 GeV,
 113 with a local significance of 4.5 standard deviations, see Fig 3. Taking the look-elsewhere effect
 114 into account in the range 110–150 GeV, this significance becomes 3.6 standard deviations. The
 115 Standard Model Higgs boson is excluded at 95% confidence level in the mass ranges of 112–123
 116 GeV and 132-143 GeV.

117 References

- 118 1. ATLAS Collaboration in *Observation of an excess of events in the search for the Stan-*
 119 *dard Model Higgs boson in the gamma-gamma channel with the ATLAS detector*, ATLAS-
 120 CONF-2012-091
- 121 2. ATLAS Collaboration in *The ATLAS Experiment at the CERN Large Hadron Collider*,
 122 *Journal of Instrumentation* **3**, S08003 (2008).
- 123 3. A. L. Read in *Presentation of search results: The CLs technique*, *J. Phys.* **G28**, 2693
 124 (2002).